

PAPER

[View Article Online](#)
[View Journal](#) | [View Issue](#)Cite this: *Mater. Adv.*, 2023,
4, 641

Insulative wood materials templated by wet foams†

Elisa S. Ferreira,^a Elizabeth Dobrzanski,^{bc} Praphulla Tiwary,^d Prashant Agrawal,^d
Richard Chen^d and Emily D. Cranston^{id} *^{ac}

Insulative materials are lightweight structures that prevent heat transfer. Plastic foams and vitreous wools are the main materials currently used for insulation in construction, although their use is associated with environmental and health concerns. In this work, lightweight solid foams (0.12 g cm^{-3}) with low thermal conductivity ($0.042 \text{ W m}^{-1} \text{ K}^{-1}$) were produced from forest residue by a green and easily scalable route. In the preparation, unrefined pine beetle-killed wood was milled and assembled as expanded structures using highly stable aqueous wet foams. The wet stability was provided by poly(vinyl alcohol) (PVA) and sodium dodecyl sulphate, which reinforced the aqueous structure and enabled the foams to be dried without significant collapse. Additionally, PVA enhanced the compressive strength and mesopore volume of the wood foams, showing that mechanical and thermal properties of wood-based insulative materials could be improved by water-soluble polymers. The structural integrity of fibre foams was maintained after exposure to high humidity, while the thermal conductivity increased with the moisture content of the materials. The materials could be fully reconstituted into foams by re-dispersing and re-foaming the components in water, which produced foams with the original density and performance. The combination of low thermal conductivity and high compressive strength indicated that wood foams can replace some of the commercially available insulation used in construction. Finally, this route to produce bio-based expanded structures from aqueous foams opens new opportunities for the development of more sustainable cellular materials without extensive mechanical/chemical refining of fibres.

Received 5th August 2022,
Accepted 7th December 2022

DOI: 10.1039/d2ma00852a

rsc.li/materials-advances

Introduction

Thermal insulation is an efficient way to reduce energy consumption in heating and cooling buildings. Vitreous wools, expanded polystyrene (EPS) and polyurethane (PU) foams are largely applied for insulation in construction, although their use is associated with numerous safety and environmental concerns.¹ For example the inhalation of fine mineral fibres is linked to acute and chronic effects on human health, particularly for workers involved in the manufacture and installation of vitreous wools.² On the other hand, the use of PS and PU in construction contributes to single use plastic production and associated difficulties in their disposal, opposing the practices of a circular economy.

Massive plastic accumulation is a global challenge with hundreds of millions of tons of plastics being disposed of annually.³ According to the International Organisation for Economic Co-operation and Development, only 9% of plastics produced worldwide is recycled after use.⁴ Furthermore, construction is the second largest sector in the production of primary plastic after the packaging industry.⁵ The use of plastics in construction generates millions of tons of waste per year and the amount disposed is expected to increase drastically.⁵

In construction, the substitution of plastics with greener alternatives, without compromising material performance is much desired need of the decade. A possible solution to meet the performance requirements is to incorporate bio-based compounds and natural raw materials into current commercial products. Greener PU foams with lignin-derived polyols can be applied in a range of cellular materials (flexible to rigid),⁶ and PU synthesized with up to 20% bio-based polyols has achieved similar performance to conventional PU.⁷ Another strategy to reduce the petrochemical-based content is to blend natural fibres with PU as composite foams.^{8,9} However, PU foams owing to their cross-linked nature lack recyclability aspect and hence impose significant strain on environment. Thus, it seems evident that the most significant improvements in sustainability may be achieved by replacing the plastic matrix (PU and PS) itself with lignocellulosic building blocks assembled as lightweight materials.

^a Department of Wood Science, University of British Columbia, Vancouver, BC, V6T 1Z4, Canada. E-mail: emily.cranston@ubc.ca

^b Bioproducts Institute, University of British Columbia, Vancouver, BC, V6T 1Z4, Canada

^c Department of Chemical and Biological Engineering, University of British Columbia, Vancouver, BC, V6T 1Z4, Canada

^d Plantee Bioplastics Inc., Vancouver, Canada

† Electronic supplementary information (ESI) available: particle size distribution, stability of wet foams and μCT 3D-reconstructed structure of wood foam (video). See DOI: <https://doi.org/10.1039/d2ma00852a>

Polymer foams are typically produced by incorporating a gas phase into polymer fluids during synthesis (e.g., PU foams) or in molten plastics (e.g., EPS and polyolefin foams),¹⁰ whereas cellulose fibre foams can be assembled by drying an aqueous foam. Scalable foam-forming processes generate fibre foams with apparent densities as low as 0.005 g cm^{-3} .¹¹ These materials are prepared by incorporating air into aqueous dispersions of fibres and surfactants, creating wet foams that are subsequently oven-dried.^{12,13} The foams are usually made from chemically refined paper grade pulps (such as bleached Kraft pulp)^{14–16} and, previously, we have shown that lightweight materials can also be produced from fibres with minor refining, such as partially delignified sugarcane bagasse (17 wt% lignin).¹⁷ In oven-dried foams, the fibres are typically assembled as expanded and open networks,¹⁸ while freeze-drying (despite being more expensive and energy intensive) may produce closed cellular structures needed for some applications.^{19,20}

The key to preparing a good thermal insulator is to assemble structures that are efficient in preventing air bone heat transfer by partitioning the gas phase within cells and mesopores.^{21,22} While cellulose fibres have been used in this regard,²³ insulative materials can also be prepared from a variety of cellulosic building blocks including microfibrillated cellulose (MFC),²⁴ cellulose nanocrystals (CNCs),²³ cellulose nanofibers (CNFs),^{22,25,26} bacterial cellulose (BC),²⁷ and regenerated cellulose (RC).^{28,29} Cellulose materials prepared by freeze-drying, supercritical drying and spray-drying achieve thermal conductivities between 0.013 and $0.075 \text{ W m}^{-1} \text{ K}^{-1}$, which is comparable to PU foams (0.020 – $0.040 \text{ W m}^{-1} \text{ K}^{-1}$)¹ and silica aerogels ($0.015 \text{ W m}^{-1} \text{ K}^{-1}$).³⁰

In this work, we have developed wood foams using pine beetle-killed (PBK) wood. PBK is a forest waste that is produced in large quantities in Canada and the United States, and its occurrence is partly linked to climate change and issues with past forest management practices.³¹ Besides the economic advantages, utilizing this forest residue has potential to remove highly flammable material and reduce the risk of forest fires. Our wood foams were 67–80 wt% milled wood (no mechanical/chemical refining) and were prepared from highly stable aqueous foam precursors containing poly(vinyl alcohol) (PVA) as a binder. The wet foams were oven-dried, creating lightweight materials (0.12 – 0.14 g cm^{-3}) with low thermal conductivities ($0.042 \text{ W m}^{-1} \text{ K}^{-1}$) and mechanical properties suitable for the replacement of insulative plastic materials in construction. Moreover, the wood foams could be fully recycled by simply re-foaming the material in water, representing a viable solution to overcome unnecessary plastic disposal in the construction sector.

Experimental

Materials

PBK wood samples were collected from Prince George (British Columbia, Canada). PVA (87–90% hydrolyzed, molecular weight $30\,000$ – $70\,000 \text{ g mol}^{-1}$), sodium dodecyl sulfate (SDS) (purity $\geq 98.5\%$), and sodium bicarbonate (purity $\geq 99.5\%$) were purchased from Sigma Aldrich. Slurries and solutions

were prepared with Millipore Milli-Q grade distilled deionized water ($18.2 \text{ M}\Omega \text{ cm}$).

PBK milling

PBK wood particles (referred to as milled wood in this work) were obtained by milling wood chips in a knife mill (SM100 Comfort, Retsch, Haan, Germany) until the particles could pass through a 1 mm mesh sieve. Wood particle size was heterogeneous with a distribution in length from $125 \mu\text{m}$ to 1 mm and aspect ratio from 2 to 12 (Fig. S1, ESI†).

Foam preparation

PVA was solubilized in water (69 mL), under magnetic stirring. After dissolving the PVA, SDS and milled wood were added to the PVA solution. The system was homogeneously dispersed with mechanical stirring and no sedimentation was observed thanks to the high viscosity of the slurry ($> 10^7 \text{ mPa s}$ at low shear rates). In sequence, the slurry (with 17.9 – 20.7 wt\% total solids content) was foamed using a homogenizer (Ultra Turrax T25, IKA, Staufen, Germany) operating at 9000 rpm , until the foam volume remained constant (*ca.* 7 min). After foaming, the wet foam was transferred to rectangular silicon molds ($33 \times 33 \text{ mm}^2$, 15 mm height, $\approx 17 \text{ mL}$) and was dried in a gravity convection oven (Isotemp, Fisherbrand, Hampton, NH, USA) overnight at 70°C . Foams were prepared with wood/PVA mass ratios of 2, 3 and 4 to evaluate the impact of PVA on the thermal and mechanical properties of the wood foams. The process has been patented under WO 2022/073126. The moisture content of the solid foams was 5.8 wt\% , as determined by gravimetric analysis after drying at 105°C . The solid contents of both the wet and dried foams are shown in Table 1.

Apparent density determination

The wood foams were weighed (as prepared from rectangular molds), and their volume was calculated using their dimensions determined using a caliper. Apparent density (ρ_{app}) is the ratio between the mass and the total volume of the foam, including both the solid phase and the voids.¹⁸

Mechanical testing

The wood foams were compressed (as prepared from rectangular molds) at 1.3 mm min^{-1} (ASTM D695) using a universal testing machine (model 5969, Instron, Norwood, MA, USA). Compressive strength was determined at 10% compression (ASTM D1621-16), and a minimum of three specimens from each group were tested. Samples were tested at room conditions (50 – 55% humidity, 23 – 24°C). Error bars shown represent the standard deviation.

Thermal conductivity

Thermal conductivity of the wood foams was determined using a thermal conductivity analyser equipped with a Modified Transient Plane Source (TCi, C-Therm, Fredericton, NB, Canada). Samples were tested at room conditions (50 – 55% humidity, 23 – 24°C).



Table 1 Composition of wet and dried wood foams prepared with wood/PVA ratios of 2, 3, and 4

| Material | Weight ratio | Solid content (wt%) | | Weight ratio | Solid content (wt%) | | Weight ratio | Solid content (wt%) | |
|----------|--------------|---------------------|----------|--------------|---------------------|----------|--------------|---------------------|----------|
| | | Wet foam | Dry foam | | Wet foam | Wet foam | | Wet foam | Dry foam |
| Wood | 2 | 13.8 | 66.5 | 3 | 14.1 | 74.8 | 4 | 14.3 | 79.7 |
| PVA | 1 | 6.9 | 33.2 | 1 | 4.7 | 24.9 | 1 | 3.6 | 19.9 |
| SDS | 0.012 | 0.1 | 0.3 | 0.012 | 0.1 | 0.3 | 0.012 | 0.1 | 0.3 |

Scanning electron microscopy (SEM)

Electron micrographs were acquired in a XL 30 microscope (Philips/FEI, Hillsboro, OR, USA) equipped with a XFlash 6110 X-ray detector (Bruker, Billerica, MA, USA), operating at 10 kV accelerating voltages. For microscopy analysis, samples were fixed on a stub with an adhesive tape and coated with carbon (*ca.* 5 nm coating) using an Auto 306 sputter (Edwards, Burgess Hill, UK).

Computed X-ray tomographic microscopy (μ CT)

A Xraia 520 Versa μ CT apparatus (Zeiss, Oberkochen, Germany) operating at 40 kV was used for acquiring 3D images of the wood foams (no staining or coating was used). Projections were collected at 5 μ m resolution (4501 projections) with an iKon-L camera equipped with a 2048 \times 2048 sensor (Andor, Belfast, Northern Ireland). Reconstructed data was analysed using the Fiji processing package for ImageJ2 freeware. Pore size analysis was conducted using the plugin MorphoLibJ for morphological segmentation. Pore size was expressed by Feret's diameter (longest distance between two points along the pore) and pore size distribution was determined as frequency from over 1000 measurements at 2D slices.

Specific surface area (SSA) and mesopore distribution

The SSA was determined using a 9-point Brunauer–Emmett–Teller (BET) method with a 3 Flex surface area analyzer (Micrometrics, Norcross, GA, USA). Before analysis, the samples (0.15–0.20 g) were kept under vacuum for 24 h at 60 °C to remove any residual moisture. SSA was determined through nitrogen sorption at a relative pressure (P_0/P) range of 0.01–0.30 and an equilibration time for sorption of 10 s. Mesopore distribution was determined using the density-functional theory (DFT) model³² fitted for a range of measurements at low relative pressure.

Water uptake test

Foams prepared with wood/PVA ratios 2, 3, and 4 were maintained at 85% humidity and 70 °C during 30 days in a humidity chamber (HCP50, Memmert), as described in the procedure B from the standard ASTM C272/C272M-18. Five samples (approx. 2.5 g) of each wood/PVA ratio were tested. The dimensions, weight and thermal conductivity of wood foams were measured prior and after the water uptake test.

Re-foamability test

Six wood foams (approx. 1.7 g each) were rewetted in water (69 mL) overnight. The slurry was re-foamed using a

homogenizer (Ultra Turrax, T25, IKA, Staufen, Germany) operating at 9000 rpm, until the foam volume remained constant (*ca.* 7 min). After foaming, the wet foams were transferred to rectangular silicon molds (33 \times 33 mm, 15 mm height, \approx 17 mL) and oven-dried in a gravity convection oven (Isotemp, Fisherbrand, Hampton, NH, USA) overnight at 70 °C. After drying, the apparent density and thermal conductivity of the recycled foams were determined.

Results and discussion

Apparent density and thermal properties of wood foams

Wood foams were prepared by foaming aqueous slurries of milled wood, PVA and SDS, and were subsequently oven-dried (Fig. 1a–c) to form rigid cellular materials (Fig. 1d). The porous structure of these wood foams was templated using highly stable wet foam precursors (Fig. S2, ESI[†]), which enabled drying with no significant structural collapse, and the generation of lightweight materials.

Different wood/PVA mass ratios were tested and the foams prepared with wood/PVA ratios of 3 and 4 had significantly lower apparent densities (0.132 ± 0.004 and 0.12 ± 0.01 g cm^{−3}, respectively) than those prepared from ratio 2 (0.142 ± 0.006 g cm^{−3}) indicating that polymer allowed for lower wood foam densities (Fig. 2). Additionally, the density of the non-foamed wood/PVA/SDS slurry after oven drying was two times higher (0.203 ± 0.005 g cm^{−3}) than that of the foamed material with identical composition, demonstrating that bubble templating through foaming is an effective way to create lightweight and porous structures.

In wood foam preparation, the milled wood provided a critical integrity to the wet structure; foams with wood particles remained expanded during drying, while foams prepared without wood particles completely collapsed into heterogeneous polymer films (Fig. 1f). On the other hand, foams prepared without PVA were fragile and exhibited a partitioning of the wood particles according to size across the vertical plane (short wood particles sedimented to the bottom and long particles rose to the top of the foam), as shown in Fig. 1g. This suggests that the PVA imparted structural integrity to the foams by acting as a “glue” and holding the wood particles together through entanglement without the need for chemical cross-linking. The combination of SDS and PVA was essential to overcome the challenge of processing unrefined milled wood through a scalable route. The additives were chosen based on wet-stability performance and commercial availability suitable for large scale applications.



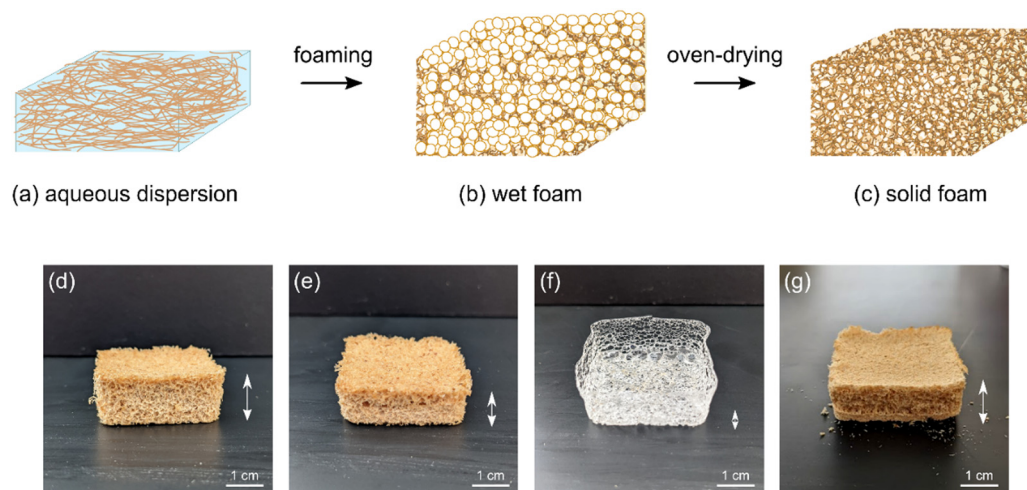


Fig. 1 Schematic representation of the preparation of wood foams: (a) aqueous slurry of milled wood, PVA and SDS; (b) aqueous wet foam precursor prepared through the incorporation of air using a homogenizer; (c) oven-dried wood foam. Macroscopic view of dried foams prepared from wood/PVA slurries with a 3 : 1 ratio (d) after foaming and oven drying, (e) a slurry dried without foaming, (f) a dried foam without milled wood, and (g) a dried foam without PVA. Arrows represent the average thickness.

The wood foams were made from milled PBK forest residue without mechanical or chemical refinement (*i.e.*, Kraft, mechanical pulping). Only mild milling of the wood was employed to decrease the particle size to a size and aspect ratio suitable for wet foam stabilization (Fig. S1, ESI†), very few individual wood fibres were liberated, the chemical composition was not altered, and substantial portions of the original wood structure were retained. Our method presents improvements in sustainability over routes that typically apply paper grade cellulose pulps and/or refined cellulose colloids (CNCs, CNFs, and RC) to produce lightweight materials. Pulping requires the isolation of cellulose fibres from lignocellulosic biomass with chemical and physical processes with relatively high energy consumption and subsequent intensive treatments are needed to produce nanocelluloses³³ and RC³⁴ from pulp. Yet, the wet foams from CNCs, CNFs and RC collapse during oven-drying, unless wet foam stability is improved by electrostatic complexation.³⁵ In this work, however, rigid wood particles provided resistance for the wet foams to avoid structural collapse and the whole biomass was applied without waste.

The structure of lightweight lignocellulosic materials is defined by its extensive hollow volume occupied by air, which imparts unique thermal properties compared to condensed lignocellulosic materials such as wood and paper.¹⁸ The expanded structure of the wood foams contributed to a low thermal conductivity, with a minimum value of $0.042 \text{ W m}^{-1} \text{ K}^{-1}$ (Fig. 2b) and no statistically significant difference between foams prepared using the three wood/PVA ratios (*i.e.*, 2, 3 and 4). In comparison, the dried, non-foamed wood/PVA/SDS slurry exhibited a higher thermal conductivity ($0.054 \text{ W m}^{-1} \text{ K}^{-1}$), as the structure was denser with the shorter wood particles sedimented to the bottom.

The thermal performance of the oven-dried wood foams was within the range of those reported for MFC foams ($0.041\text{--}0.047 \text{ W m}^{-1} \text{ K}^{-1}$),²⁴ nanocellulose materials prepared

by freeze-drying and critical point drying ($0.013\text{--}0.075 \text{ W m}^{-1} \text{ K}^{-1}$),¹⁸ and close to that of commercially available insulation materials such as PU foams, EPS, and stone wools as compared in. Overall, there are only a few examples of oven-dried cellulosic materials with thermal insulative performance because the pore structure is collapsed at ambient drying. The reported oven-dried cellulosic materials are composites with silica and polyoxamer-based foams with a network sufficiently strong to be oven-dried.³⁶ We believe that to ensure low cost and scalable processing for the construction and packaging industries, that avoiding freeze-drying and critical point drying is pertinent.

Wood foam structure and mesopore distribution

The morphology and pore size distribution of the wood foams was investigated using μ CT, SEM and nitrogen sorption, exhibiting a hierarchical pore size distribution with widths ranging from nanometres to millimetres. Images from μ CT revealed expanded wood networks (Fig. 3a and b) with porosity of 90.7%, as determined by the ratio of voxels from the background noise (air) and solid phase.

The large pores characterized by μ CT can be classified as open cells with widths between 0.1 and 2.4 mm (Fig. 3g). Cross-sectional images showed that the wood particles were randomly oriented and connected by a few contact points between wood particles, forming open polyhedral cells (Fig. 3c, d and video S1 in ESI†). In aqueous foams, the walls of the cells are typically assembled as polygons, as the liquid film from plateau borders (liquid layer separating bubbles) is drained and/or evaporated resulting in spherical bubbles becoming polyhedral with flattened liquid films.³⁷

Moreover, μ CT images elucidated the honeycomb structure of wood with pore width ranging from 20 to 50 μm (Fig. 3e and f); we suspect these pores contribute significantly to the good thermal insulation performance.³⁶ The lack of mechanical and chemical refining of the PBK wood in this work allows for



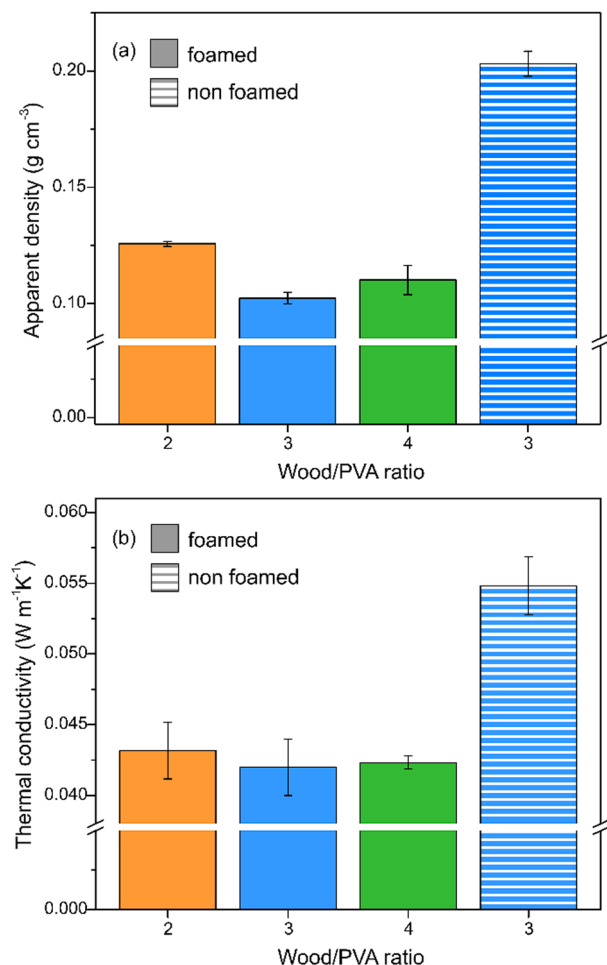


Fig. 2 (a) Apparent density and (b) thermal conductivity of dried wood foams prepared from slurries with different wood/PVA ratios with (slanted lines) and a control sample prepared by oven drying the slurry without foaming (horizontal lines).

naturally hierarchical structures in the foams and enhanced functionally. For example, in addition to the reduced thermal conductivity, the porous framework of wood is a valuable scaffold for composites where nano and micro structures, and well-aligned cellulose fibres lead to anisotropic mechanical properties, as previously shown in bio-based polyethylene composites.³⁸

SEM analysis showed that the milled wood particles had assembled in a tetrahedral framework upon the removal of water (Fig. 4a), which is characteristic of dry foams.³⁷ The framework is formed by open cells reinforced by wood joints and milled wood assemblies “glued” together by PVA (Fig. 4b and c). Overall, the expanded morphology of the wood foams is a combination of open polyhedral cells with sizes (and size distributions) restricted by the rigid milled wood, which were originally located at the plateau borders around air bubbles.

In addition to the large air-bubble-templated open cells and honeycomb pores from wood, the wood foams also had pores within the mesopore size range (*i.e.*, 2–50 nm) as detected by nitrogen gas sorption experiments. Foams with a wood/PVA

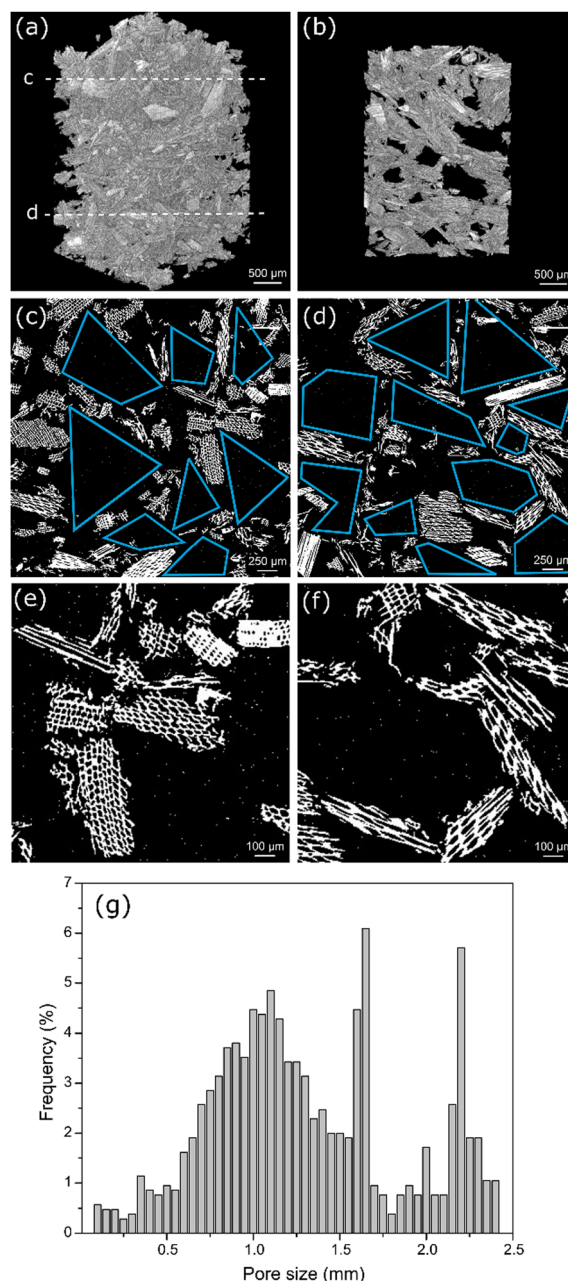


Fig. 3 Reconstructed μ CT images of a wood foam prepared with a wood/PVA ratio of 3 showing (a and b) 3D-overview; (c and d) cross-sections from (a) with polyhedral cells highlighted in blue; (e and f) cross-sections showing the honeycomb structures of the wood cell wall; (g) pore size distribution from morphological segmentation. See video ESI,† for the 3D rendering of panel (a).

ratio of 2 had a larger volume of mesopores (Fig. 5a) than those with ratios of 3 and 4. As such, it seems that PVA is responsible for the mesopores and while more PVA makes a slightly denser structure (Fig. 2a) more mesopores likely reduce the thermal conductivity which explains how a denser foam can have the same thermal conductivity as a less dense foam (Fig. 2b).

The beneficial role of mesopores in thermal insulation was previously demonstrated for CNF cryogels that had an extremely low thermal conductivity ($0.022 \text{ W m}^{-1} \text{ K}^{-1}$) and pore

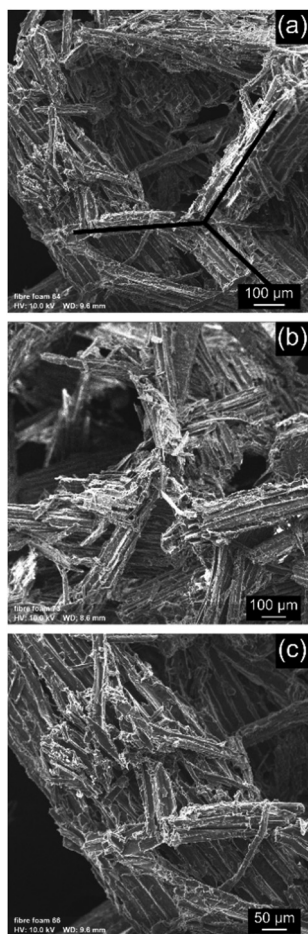


Fig. 4 SEM images of the wood foams exhibiting (a) cellular pores with milled wood assembled as a tetrahedral framework; (b) wood-PVA interlocked structures formed from milled wood with widths $< 50 \mu\text{m}$, (c) short milled wood particles ($< 500 \mu\text{m}$ long) assembled along the surface of longer milled wood particles ($> 800 \mu\text{m}$ long).

sizes between 2 and 100 nm.²² Overall, it was evident that more PVA and more mesopores led to larger specific surface area

values (Fig. 5b). Because the wood foams were prepared using unrefined milled wood and oven-drying (where capillary forces still play a major role), their SSA values were relatively low; the highest surface area foam was the wood/PVA ratio 2 that had an SSA of $2.04 \text{ m}^2 \text{ g}^{-1}$. Regardless, they were comparable to some other foams and aerogels prepared by oven and/or ambient drying from RC ($0.81 \text{ m}^2 \text{ g}^{-1}$),³⁹ cellulose fibres ($4\text{--}8 \text{ m}^2 \text{ g}^{-1}$),¹⁵ and CNFs ($4\text{--}10 \text{ m}^2 \text{ g}^{-1}$),³⁹ and even some freeze-dried gels from CNFs ($1 \text{ m}^2 \text{ g}^{-1}$),²⁵ CNCs ($17 \text{ m}^2 \text{ g}^{-1}$),⁴⁰ and RC ($23 \text{ m}^2 \text{ g}^{-1}$).³⁹

Mechanical properties of solid wood foams

The wood foams exhibited a mechanical response typical of lightweight materials; the compressive stress-strain curves showed distinct (I) elastic, (II) plateau, and (III) densification regions (Fig. 6a).¹² The wood foams prepared with wood/PVA ratios of 2 and 3 had compressive strengths significantly higher than those prepared with a ratio of 4 (Fig. 6b), indicating that the structure of the wood foams was reinforced by PVA. In fibre materials such as paper and foams, resistance to mechanical stress is provided by fibre-fibre contact points, which is mainly linked to the connecting interfacial area between fibres.^{41,42} In the wood foams studied here, PVA acted as a binder connecting milled wood particles and enhancing the interfacial contact area and the mechanical resistance of contact points by polymer entanglements, without the need for chemical cross-linking. The compressive strength of the rigid wood foams (up to $43.9 \pm 0.7 \text{ kPa}$), was within the range of previously reported nanocellulose aerogels and foams ($10\text{--}70 \text{ kPa}$),¹⁸ while highly entangled cellulose networks of MFC foams have higher strengths ($69\text{--}190 \text{ kPa}$).²⁴ Commercially available insulation materials such as EPS and PU foams have a broad range of mechanical properties and can range from flexible to extremely rigid (with compressive strengths from 2 to 48 000 kPa, respectively),⁴³ while vitreous wools are highly brittle and have no resistance to mechanical stresses.

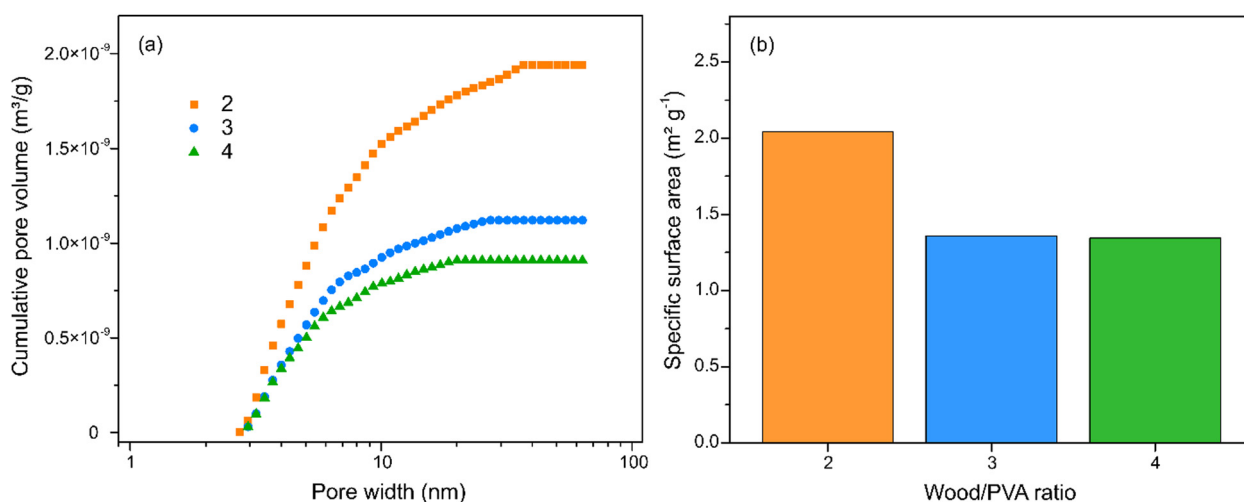


Fig. 5 Mesoporosity and surface area of dried wood foams prepared at wood/PVA ratios of 2, 3, and 4 as determined by nitrogen gas sorption: (a) cumulative pore volume as a function of pore width obtained by DFT modelling; (b) SSA determined by BET analysis.



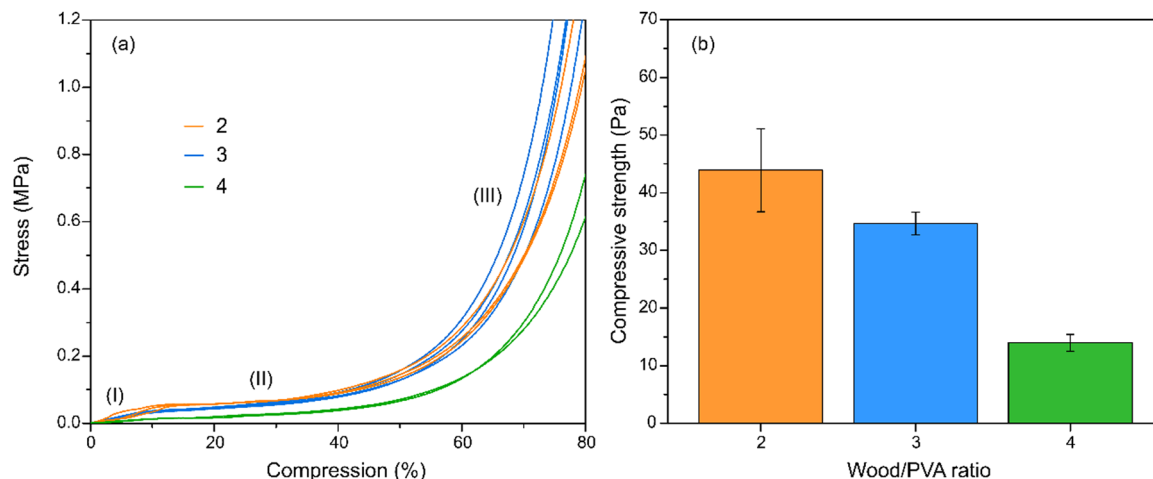


Fig. 6 Mechanical properties of wood foams prepared with wood/PVA ratios of 2, 3, and 4: (a) stress–strain diagrams under compressive strain showing three compressive regions: (I) elastic, (II) plateau, and (III) densification; (b) compressive strength at 10% compression according to ASTM Standard (D1621-16).

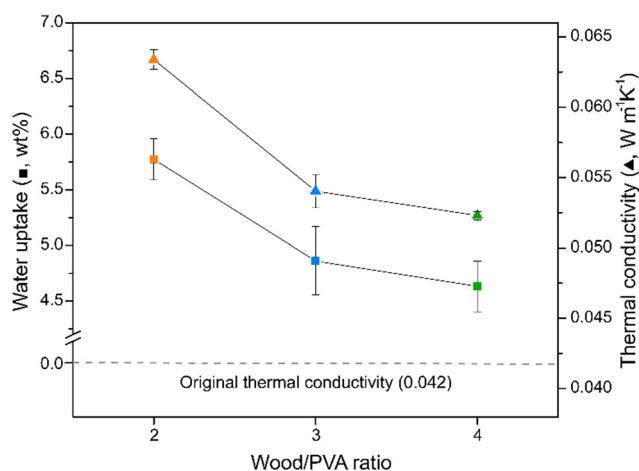


Fig. 7 Water uptake (squares) and thermal conductivity (triangles) of wood foams prepared with wood/PVA ratios 2, 3, and 4, after conditioning at 85% humidity and 70 °C for 30 days.

The mechanical and thermal properties of the wood foams suggest that these materials could be used as a bio-based panelling for thermal insulation in civil construction and vehicles to replace plastic foams. In addition to their thermal insulation, the wood foams may exhibit a similar sound absorption capacity as previously shown for foams from paper-grade pulp.¹⁴ These foams could thus be potentially used as panels to provide acoustic comfort. Moreover, due to their insulative nature and mechanical strength, the wood foams may also find use in applications replacing EPS packaging.

Correlation between water uptake and thermal conductivity

A water absorption test was carried out at high humidity (85%, 70 °C) for 30 days, according to ASTM C272/C272M-18. The water uptake was dependent of the wood foam composition, being inversely proportional to the wood/PVA ratio (Fig. 7). The results showed that PVA favoured water absorption and the

water uptake ranged from 5.8 to 4.6 wt% for wood/PVA ratios 2 and 4, respectively. Moreover, we observed that the thermal conductivity increased with the water uptake from 0.042 to 0.063 m⁻¹ K⁻¹ for the maximum water uptake (foam with wood/PVA ratio 4).

The thermal conductivity of hygroscopic insulative materials is expressed as a linear function of the volumetric water content by Künzle's model.⁴⁴ Moisture affects the performance of cellulose-based insulation, as reported for loose fill cellulose fibres⁴⁵ and CNF oven-dried foams,⁴⁶ and mineral fibrous insulation (fibre glass and rock wools).⁴⁷ Further investigation is needed to elucidate mechanisms for reducing the heat transfer in cellulose at high humidity.³⁶ To keep the original low thermal conductivity, the foams could be protected in the core of laminate structures, which are already used in constructions. For instance, EPS borders are sandwiched between thermoplastic-glass materials or concrete frames and walls.^{48,49} Hydrophobic agents (e.g. waxes) could also be used to prevent water uptake; however, the dispersibility and foamability of the wet slurry would be reduced, compromising large scale applications.

In the wood foams, there were no significant structural differences after being exposed to high humidity for 30 days. The structural integrity was maintained and the samples retained their original dimensions, as the water uptake was relatively low (ca. 5 wt%). Additionally, the rigidity of the wood foams was similar after the water uptake test, indicating that there were no changes in the compressive strength (see video S2 and S3, ESI†).

Re-foamability of wood foams

Although the structural integrity of the wood foams was kept at high humidity, the foams were easily dispersed after immersion in water. The wood foams could be fully reconstituted into foams by re-dispersing and re-foaming the components in water, followed by oven drying (Fig. 8), to reproducing foams



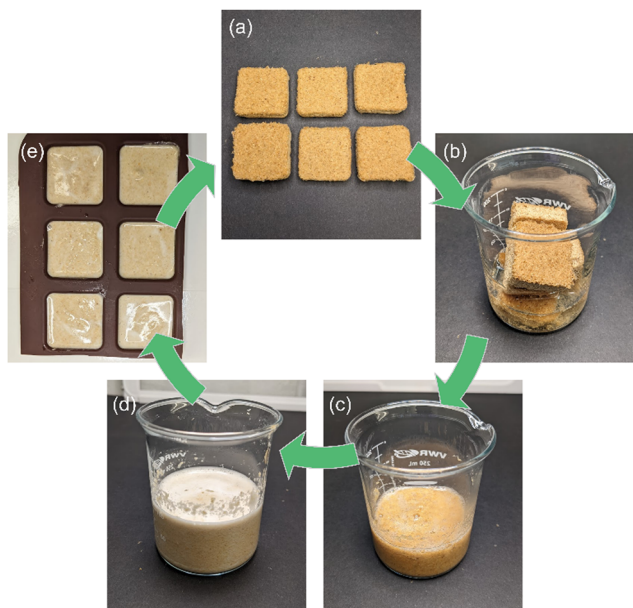


Fig. 8 Re-foamability test showing (a) dried wood foams; (b) wood foams being soaked in water, (c) re-wetted and mixed wood foams forming a slurry that is indistinguishable from the original, (d) re-foamed wood slurry; (e) re-foamed wet wood foams in silicone molds prior to oven-drying – dried foams are also indistinguishable from the originals.

with the original density and thermal conductivity ($0.13 \pm 0.03 \text{ g cm}^{-3}$ and $0.0442 \pm 0.0004 \text{ W m}^{-1} \text{ K}^{-1}$ for “remade” foams, $0.132 \pm 0.004 \text{ g cm}^{-3}$ and $0.042 \pm 0.002 \text{ W m}^{-1} \text{ K}^{-1}$, for “freshly” prepared foams). Foam recyclability without further processing was possible because dismantling the water-soluble supramolecular structures of PVA and SDS is a simple dissolution process.

The lack of wet strength of cellulosic networks is well-known in the literature, and much work is carried out to impart wet strength through chemical and physical cross-linking or surface modification with hydrophobes.^{12,42} In this work, however, instead of attempting to overcome cellulose hydrophilicity, we see the lack of wet strength as an advantage due to the ease of recyclability. The additives were applied targeting recyclability as there is an urgent demand for recyclable and bio-based materials to replace plastics in construction.⁵⁰ More sustainable additives (natural surfactants and biopolymers) can be used in future work, and their application can become feasible if costs are overcome by regulations that benefit green products.

For construction applications, the natural properties of cellulosic materials such as susceptibility to moisture, biodegradation and high flammability can be overcome with numerous strategies that have been successfully applied to both cellulose and plastics. To impart flame-retardancy to these materials, the incorporation of sodium bicarbonate,⁵¹ nanoclay,²⁴ polyelectrolyte multilayers^{52,53} or cellulose phosphorylation are efficient strategies.⁵⁴ Finally, the microbial activity of cellulosic materials can be reduced, when desired, without compromising their eco-friendly aspects by using positively-charged celluloses,^{55–57} chitosan,⁵⁸ or nisin.^{59,60}

Conclusions

Insulative wood materials with a porous cellular structure were prepared by oven drying a foamed slurry of predominantly milled wood with water-soluble polymers and surfactants. Solid wood foams from unrefined wood exhibited low densities (0.12 g cm^{-3}) and thermal conductivities close to commercially available insulative materials typically used in construction ($0.042 \text{ W m}^{-1} \text{ K}^{-1}$). Moreover, the compressive strength, water uptake and mesopore volume of the foams were increased by increasing the PVA content, indicating that mechanical and thermal properties of insulative wood foams can be tailored by the incorporation of water-soluble polymers.

In addition to the performance of the solid foams, the combination of rigid wood particles and polymer entanglements was central to produce wet foam precursors with sufficient stability to be oven-dried. The presence of a water-soluble polymer and dispersible wood “colloids” also allowed for the pristine foam components to be fully recovered and reassembled into new foams with similar densities and thermal performance. While the foams can be recycled when immersed in water, the structural integrity was not changed by exposure to high humidity. Therefore, this preparation route for bio-based foams presents a significant improvement in sustainability for the design of novel, recyclable cellular materials from unrefined wood and forest residues.

Author contributions

E. S. F.: conceptualization, writing – original draft, writing – review & editing, investigation, visualization, methodology, funding acquisition, project administration. E. D.: conceptualization, writing – original draft, writing – review & editing, investigation, methodology. P. T.: conceptualization, writing – review & editing, visualization, methodology, funding acquisition, project administration. P. A.: conceptualization, writing – review & editing, visualization, methodology, funding acquisition, project administration. R. C.: conceptualization, writing – review & editing, investigation, visualization, funding acquisition, project administration. E. C.: conceptualization, writing – original draft, writing – review & editing, visualization, supervision, project administration, funding acquisition.

Conflicts of interest

There are no conflicts to declare.

Acknowledgements

The authors thank Dr Elina Niinivaara for proofreading, James Drummond (PPC) for μCT imaging, Prof. Shahabaddine Sokhansanj, Prof. Scott Renneckar, Prof. Feng Jiang, Prof. Orlando Rojas, Prof. Mark Martinez, Saeid Soltanian (AMPEL), and Jacob Kabel (EMXDF) for equipment usage. Plantee Bioplastics acknowledges funding from Natural Resources Canada (NRCAN, 2019-F0041-C00001) and the authors acknowledge the



Natural Sciences and Engineering Research Council of Canada (RGPIN-2018-06818). E. S. F. thanks Mitacs and Plantee Bioplastics (Mitacs Accelerate, IT22973 and IT30768). E. D. C. is grateful for support and recognition through the University of British Columbia's President's Excellence Chair initiative, the NSERC E.W.R. Steacie Memorial Fellowship and the Canadian Foundation for Innovation (John R. Evans Leaders Fund) for equipment.

Notes and references

- 1 S. Schiavoni, F. D'Alessandro, F. Bianchi and F. Asdrubali, Insulation materials for the building sector: A review and comparative analysis, *Renewable Sustainable Energy Rev.*, 2016, **62**, 988–1011.
- 2 United States Environmental Protection Agency, Fine Mineral Fibers Hazard Summary, <https://www.epa.gov/sites/default/files/2016-10/documents/fine-mineral-fibers.pdf>, (accessed 6 January 2022).
- 3 S. Kaza, L. C. Yao, P. Bhada-Tata and F. van Woerden, *What a Waste 2.0*, World Bank, Washington, DC, 2018.
- 4 Plastic pollution is growing relentlessly as waste management and recycling fall short, says OECD, <https://www.oecd.org/environment/plastic-pollution-is-growing-relentlessly-as-waste-management-and-recycling-fall-short.htm>, (accessed 14 July 2022).
- 5 R. Geyer, J. R. Jambeck and K. L. Law, Production, use, and fate of all plastics ever made, *Sci. Adv.*, 2017, **3**, e1700782.
- 6 J. Peyrton and L. Avérous, Structure-properties relationships of cellular materials from biobased polyurethane foams, *Mater. Sci. Eng., R*, 2021, **145**, 100608.
- 7 P. Mukhopadhyaya, M. T. Ton-That, T. D. Ngo, N. Legros, J. F. Masson, S. Bundalo-Perc and D. van Reenen, An investigation on bio-based polyurethane foam insulation for building construction, ASTM Special Technical Publication, 2014, 1574, 131–141.
- 8 R. Gu, M. M. Sain and S. K. Konar, A feasibility study of polyurethane composite foam with added hardwood pulp, *Ind. Crops Prod.*, 2013, **42**, 273–279.
- 9 C. Kuranchie, A. Yaya and Y. D. Bensah, The effect of natural fibre reinforcement on polyurethane composite foams – A review, *Sci. Afr.*, 2021, **11**, e00722.
- 10 P. S. Liu and G. F. Chen, Producing Polymer Foams, *Porous Mater.*, 2014, 345–382.
- 11 M. Alimadadi and T. Uesaka, 3D-oriented fiber networks made by foam forming, *Cellulose*, 2016, **23**, 661–671.
- 12 E. S. Ferreira, C. A. Rezende and E. D. Cranston, Fundamentals of cellulose lightweight materials: bio-based assemblies with tailored properties, *Green Chem.*, 2021, **23**, 3542–3568.
- 13 T. Hjelt, J. A. Ketoja, H. Kiiskinen, A. I. Koponen and E. Pääkkönen, Foam forming of fiber products: a review, *J. Dispers. Sci. Technol.*, 2022, **43**, 1462–1497.
- 14 T. Pöhler, P. Jetsu and H. Isomoisio, Benchmarking new wood fibre-based sound absorbing material made with a foam-forming technique, *Build. Acoust.*, 2016, **23**, 131–143.
- 15 E. S. Ferreira and C. A. Rezende, Simple Preparation of Cellulosic Lightweight Materials from Eucalyptus Pulp, *ACS Sustainable Chem. Eng.*, 2018, **6**, 14365–14373.
- 16 S. R. Burke, M. E. Möbius, T. Hjelt and S. Hutzler, Properties of lightweight fibrous structures made by a novel foam forming technique, *Cellulose*, 2019, **26**, 2529–2539.
- 17 E. S. Ferreira, E. D. Cranston and C. A. Rezende, Naturally Hydrophobic Foams from Lignocellulosic Fibers Prepared by Oven-Drying, *ACS Sustainable Chem. Eng.*, 2020, **8**, 8267–8278.
- 18 E. S. Ferreira, C. A. Rezende and E. D. Cranston, Fundamentals of cellulose lightweight materials: bio-based assemblies with tailored properties, *Green Chem.*, 2021, **23**, 3542–3568.
- 19 Z. Hu, R. Xu, E. D. Cranston and R. H. Pelton, Stable Aqueous Foams from Cellulose Nanocrystals and Methyl Cellulose, *Biomacromolecules*, 2016, **17**, 4095–4099.
- 20 S. Tasset, B. Cathala, H. Bizot and I. Capron, Versatile cellular foams derived from CNC-stabilized Pickering emulsions, *RSC Adv.*, 2013, **4**, 893–898.
- 21 L. J. Gibson and M. F. Ashby, *Cellular Solids: Structure and Properties*, Cambridge University Press, 2 edn, 1997.
- 22 K. Sakai, Y. Kobayashi, T. Saito and A. Isogai, Partitioned air at microscale and nanoscale: thermal diffusivity in ultrahigh porosity solids of nanocellulose, *Sci. Rep.*, 2016, **6**, 20434.
- 23 B. Seantier, D. Bendahou, A. Bendahou, Y. Grohens and H. Kaddami, Multi-scale cellulose based new bio-aerogel composites with thermal super-insulating and tunable mechanical properties, *Carbohydr. Polym.*, 2016, **138**, 335–348.
- 24 C. Zheng, D. Li and M. Ek, Improving fire retardancy of cellulosic thermal insulating materials by coating with bio-based fire retardants, *Nord. Pulp Pap. Res. J.*, 2019, **34**, 96–106.
- 25 C. Jiménez-Saelices, B. Seantier, B. Cathala and Y. Grohens, Spray freeze-dried nanofibrillated cellulose aerogels with thermal superinsulating properties, *Carbohydr. Polym.*, 2017, **157**, 105–113.
- 26 Kobayashi Yuri, Saito Tsuguyuki and Isogai Akira, Aerogels with 3D Ordered Nanofiber Skeletons of Liquid-Crystalline Nanocellulose Derivatives as Tough and Transparent Insulators, *Angew. Chem., Int. Ed.*, 2014, **53**, 10394–10397.
- 27 B. Fleury, E. Abraham, J. A. de La Cruz, V. S. Chandrasekar, B. Senyuk, Q. Liu, V. Cherpak, S. Park, J. B. ten Hove and I. I. Smalyukh, Aerogel from Sustainably Grown Bacterial Cellulose Pellicles as a Thermally Insulative Film for Building Envelopes, *ACS Appl. Mater. Interfaces*, 2020, **12**, 34115–34121.
- 28 I. Karadagli, B. Schulz, M. Schestakow, B. Milow, T. Gries and L. Ratke, Production of porous cellulose aerogel fibers by an extrusion process, *J. Supercrit. Fluids*, 2015, **106**, 105–114.
- 29 J. Feng, S. T. Nguyen, Z. Fan and H. M. Duong, Advanced fabrication and oil absorption properties of super-hydrophobic recycled cellulose aerogels, *Chem. Eng. J.*, 2015, **270**, 168–175.
- 30 A. C. Pierre and G. M. Pajonk, Chemistry of Aerogels and Their Applications, *Chem. Rev.*, 2002, **102**, 4243–4266.
- 31 F. Larock, *The potential of increasing the use of BC forest residues for bioenergy and biofuels*, University of British Columbia, 2018.



- 32 R. Bardestani, G. S. Patience and S. Kaliaguine, Experimental methods in chemical engineering: specific surface area and pore size distribution measurements—BET, BJH, and DFT, *Can. J. Chem. Eng.*, 2019, **97**, 2781–2791.
- 33 H. Kargarzadeh, I. Ahmad, S. Thomas and A. Dufresne, *Handbook of Nanocellulose and Cellulose Nanocomposites*, John Wiley & Sons., 2017, 2 Volume Set.
- 34 A. J. Sayyed, N. A. Deshmukh and D. v Pinjari, A critical review of manufacturing processes used in regenerated cellulosic fibres: viscose, cellulose acetate, cuprammonium, LiCl/DMAc, ionic liquids, and NMMO based lyocell, *Cellulose*, 2019, **26**, 2913–2940.
- 35 N. T. Cervin, E. Johansson, J.-W. Benjamins and L. Wågberg, Mechanisms Behind the Stabilizing Action of Cellulose Nanofibrils in Wet-Stable Cellulose Foams, *Biomacromolecules*, 2015, **16**, 822–831.
- 36 V. Apostolopoulou-Kalkavoura, P. Munier and L. Bergström, Thermally Insulating Nanocellulose-Based Materials, *Adv. Mater.*, 2020, 2001839.
- 37 D. Langevin, Aqueous foams: A field of investigation at the Frontier between chemistry and physics, *ChemPhysChem*, 2008, **9**, 510–522.
- 38 R. L. Pereira Oliveira Moreira, J. A. Simão, R. F. Gouveia and M. Strauss, Exploring the Hierarchical Structure and Alignment of Wood Cellulose Fibers for Bioinspired Anisotropic Polymeric Composites, *ACS Appl. Bio. Mater.*, 2020, **3**, 2193–2200.
- 39 K. Ganesan, A. Dennstedt, A. Barowski and L. Ratke, Design of aerogels, cryogels and xerogels of cellulose with hierarchical porous structures, *Mater. Des.*, 2016, **92**, 345–355.
- 40 M. Fumagalli, D. Ouhab, S. M. Boisseau and L. Heux, Versatile Gas-Phase Reactions for Surface to Bulk Esterification of Cellulose Microfibrils Aerogels, *Biomacromolecules*, 2013, **14**, 3246–3255.
- 41 M. Alava and K. Niskanen, The physics of paper, *Rep. Prog. Phys.*, 2006, **69**, 669.
- 42 T. Lindström and L. Wågberg, On the nature of joint strength in paper-A review of dry and wet strength resins in paper manufacturing, 13th Fundamental Research Symposium, 2005, 457–562.
- 43 MatWeb - The Online Materials Information Resource, <https://www.matweb.com/search/QuickText.aspx?SearchText=Material%20Property%20Data> (accessed 2022-05-19).
- 44 H. M. Künzel and K. Kiessl, Calculation of heat and moisture transfer in exposed building components, *Int. J. Heat Mass Transfer*, 1996, **40**, 159–167.
- 45 S. Vėjelis, I. Gnipas and V. Keršulis, Performance of Loose-Fill Cellulose Insulation, *Mater. Sci.*, 2006, **12**, 338–340.
- 46 V. Apostolopoulou-Kalkavoura, K. Gordeyeva, N. Lavoine and L. Bergström, Thermal conductivity of hygroscopic foams based on cellulose nanofibrils and a nonionic polyoxamer, *Cellulose*, 2018, **25**, 1117–1126.
- 47 A. Abdou and I. Budaiwi, The variation of thermal conductivity of fibrous insulation materials under different levels of moisture content, *Constr. Build. Mater.*, 2013, **43**, 533–544.
- 48 P. L. N. Fernando, M. T. R. Jayasinghe and C. Jayasinghe, Structural feasibility of Expanded Polystyrene (EPS) based lightweight concrete sandwich wall panels, *Constr. Build. Mater.*, 2017, **139**, 45–51.
- 49 M. A. Mousa and N. Uddin, Flexural Behavior of Full-Scale Composite Structural Insulated Floor Panels, *Adv. Compos. Mater.*, 2011, **20**, 547–567.
- 50 Plastics Challenge: Development of Next Generation Bio-Based Foam Insulation - Innovative Solutions Canada, <https://www.ic.gc.ca/eic/site/101.nsf/eng/00066.html>, (accessed 6 March 2022).
- 51 M. Farooq, M. H. Sipponen, A. Seppälä and M. Österberg, Eco-friendly Flame-Retardant Cellulose Nanofibril Aerogels by Incorporating Sodium Bicarbonate, *ACS Appl. Mater. Interfaces*, 2018, **10**, 27407–27415.
- 52 T. J. Kolibaba and J. C. Grunlan, Environmentally Benign Polyelectrolyte Complex That Renders Wood Flame Retardant and Mechanically Strengthened, *Macromol. Mater. Eng.*, 2019, **304**, 1900179.
- 53 O. Köklükaya, F. Carosio, J. C. Grunlan and L. Wågberg, Flame-Retardant Paper from Wood Fibers Functionalized via Layer-by-Layer Assembly, *ACS Appl. Mater. Interfaces*, 2015, **7**, 23750–23759.
- 54 B. G. Fiss, L. Hatherly, R. S. Stein, T. Friščić and A. Moores, Mechanochemical Phosphorylation of Polymers and Synthesis of Flame-Retardant Cellulose Nanocrystals, *ACS Sustain. Chem. Eng.*, 2019, **7**, 7951–7959.
- 55 C. G. Otoni, J. S. L. Figueiredo, L. B. Capeletti, M. B. Cardoso, J. S. Bernardes and W. Loh, Tailoring the Antimicrobial Response of Cationic Nanocellulose-Based Foams through Cryo-Templating, *ACS Appl. Bio. Mater.*, 2019, **2**, 1975–1986.
- 56 J. A. Sirviö, A. K. Anttila, A. M. Pirttilä, H. Liimatainen, I. Kilpeläinen, J. Niinimäki and O. Hormi, Cationic wood cellulose films with high strength and bacterial anti-adhesive properties, *Cellulose*, 2014, **21**, 3573–3583.
- 57 A. Chaker and S. Boufi, Cationic nanofibrillar cellulose with high antibacterial properties, *Carbohydr. Polym.*, 2015, **131**, 224–232.
- 58 A. Ottenhall, T. Seppänen and M. Ek, Water-stable cellulose fiber foam with antimicrobial properties for bio based low-density materials, *Cellulose*, 2018, **25**, 2599–2613.
- 59 M. Tavakolian, M. Okshevsky, T. G. M. van de Ven and N. Tufenkji, Developing Antibacterial Nanocrystalline Cellulose Using Natural Antibacterial Agents, *ACS Appl. Mater. Interfaces*, 2018, **10**, 33827–33838.
- 60 R. Weishaupt, L. Heuberger, G. Siqueira, B. Gutt, T. Zimmermann, K. Maniura-Weber, S. Salentinig and G. Faccio, Enhanced Antimicrobial Activity and Structural Transitions of a Nanofibrillated Cellulose-Nisin Biocomposite Suspension, *ACS Appl. Mater. Interfaces*, 2018, **10**, 20170–20181.

